

실제 SAR 영상에 대한 위상 확장 역필터링의 적용

도대원, 송우진, 권준찬

포항공과대학교 전자컴퓨터공학부 전자파연구센터

PHASE-EXTENSION INVERSE FILTERING ON REAL SAR IMAGES

Dae-Won Do, Woo-Jin Song and Jun-Chan Kwon

Microwave Application Research Center, Division of Electronics & Computer Engineering
Pohang University of Science and Technology

ABSTRACT

Through matched filtering synthetic aperture radar (SAR) produces high-resolution imagery from data collected by a relative small antenna. While the impulse response obtained by the matched filter approach produces the best achievable signal-to-noise ratio, large sidelobes must be reduced to obtain higher-resolution SAR images. So, many enhancement methods of SAR imagery have been proposed. As a deconvolution method, the phase-extension inverse filtering is based on the characteristics of the matched filtering used in SAR imaging. It improves spatial resolution as well as effectively suppresses the sidelobes with low computational complexity. In the phase-extension inverse filtering, the impulse response is obtained from simulation with a point target. But in a real SAR environment, for example ERS-1, the impulse response is distorted by many non-ideal factors. So, in the phase-extension inverse filtering for a real SAR processing, the magnitudes of the frequency transfer function have to be compensated to produce more desirable results. In this paper, an estimation method to obtain a more accurate impulse response from a real SAR image is studied. And a compensation scheme to produce better performance of the phase-extension inverse filtering is also introduced.

1. INTRODUCTION

Synthetic aperture radar (SAR) is a microwave imaging system capable of producing high-resolution imagery from data collected by a relative small antenna [1]. Due to these advantages, SAR has been used for various purposes such as earth surface observation, ocean observation, natural resources detection, and planetary detection. Conventionally, SAR images are reconstructed from received data by matched filter approach. Though the impulse response obtained by the matched filter approach produces the best achievable signal-to-noise ratio, high sidelobes must be reduced to obtain higher-resolution SAR images. To overcome the classical limit

of the matched filter approach, recently many enhancement techniques are proposed, so called super-resolution techniques [3][4]. In general, super-resolution is a commonly used term for techniques which allow resolution beyond the diffraction limit in coherent imaging systems, such as SAR system.

As an enhancement method, phase-extension inverse filtering [5] is based on the characteristics of the matched filtering used in SAR imaging. It improves spatial resolution as well as effectively suppresses the sidelobes with low computational complexity; its performance for simulated SAR image is presented in [5]. In the simulation, the impulse response is obtained from a point target under ideal situation and its transfer function is used. But in a real SAR environment, the impulse response is distorted by many non-ideal factors. Therefore in the phase-extension inverse filtering for a real SAR processing, the magnitudes of the frequency transfer function have to be compensated to produce more desirable results. And to apply the transfer function to real SAR images practical problems are considered, such as Doppler frequency drift and depth of focus.

In this paper, an estimation method to obtain a more accurate impulse response from a real SAR image is studied. And a compensation method to produce better performance of the phase-extension inverse filtering in a real SAR environment is also introduced.

The rest of this paper is organized as follows. Section 2 reviews the phase-extension inverse filtering and describes considerations when we apply it to real SAR images. In Section 3, we describe the method of obtaining an impulse response in a real SAR images. Section 4 shows the experimental result processed by compensated magnitudes of transfer function. Finally, Section 5 presents a summary and conclusions.

2. PHASE-EXTENSION INVERSE FILTERING

According to the partition of the transfer function in Fig.

1, the phase extension inverse filtering is formulated as

$$\text{Domain 1 } (|G(u, v)| > T): \hat{X}(u, v) = \frac{\tilde{X}(u, v)}{|G(u, v)|}, \quad (1)$$

$$\text{Domain 2 } (|G(u, v)| < T): \hat{X}(u, v) = \begin{cases} \frac{\tilde{X}(u, v)}{|\tilde{X}(u, v)|} \times \eta C, & \text{if } |\tilde{X}(u, v)| > \sigma, \\ 0.0, & \text{elsewhere} \end{cases} \quad (2)$$

where $G(u, v)$ is the 2-D transfer function, $\tilde{X}(u, v)$ is the spectrum of the matched filtered SAR image and T is a threshold which corresponds to the predetermined signal bandwidth.

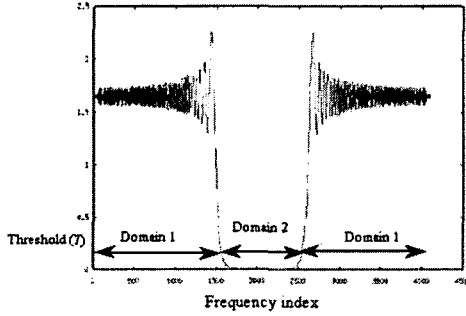


Fig. 1. The partition of the transfer function.

In Eqn. (1) the magnitude inverse filtering is processed to get a more sinc-like impulse response, which retains the phase information to make the phase component in the Domain 1 continuous to that in the Domain 2. And in the Domain 2 the magnitude level is adjusted to get the proper effect of extending bandwidth. Parameter C and the system parameter η is used to adjust the magnitude level as In Eqn. (2). And σ is a control parameter for computational precision, which prevents the division by zero. The parameter C is the average magnitude of the spectrum of the matched filtered data, which is defined by

$$C = \frac{\sum_{u=0}^{N-1} \sum_{v=0}^{M-1} |\tilde{X}(u, v)|}{MN}, \quad (3)$$

where M, N represent the size of FFT in each direction of azimuth and range, respectively. Note that as the variance of the noise increases, the value of C also increases. In Eqn. (2) the system parameter η prevents the effect of the added noise from being larger than that of the desired signal of reflectivity, that is, noise enhancement. Thus the value of η is set to be inversely

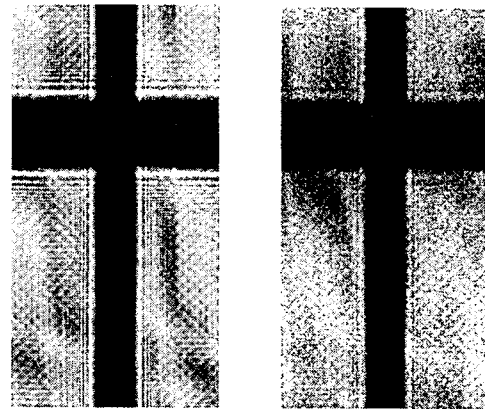
proportional to the variance of the added noise to prevent the noise enhancement. The relation between η and the noise can be expressed as

$$\eta = \frac{K}{\text{var}\{n(i, j)\}}, \quad (4)$$

where K is an inverse ratio which is chosen empirically.

As indicated in Eqn. (1) and Eqn. (2), the phase-extension inverse filtering extends the bandwidth of controlling the magnitude components of $\tilde{X}(u, v)$ without affecting the phase components of that. Since the phase distortion in the frequency domain corresponds to a displacement in the spatial domain, they may degrade the spatial resolution. So the phase-extension inverse filtering retains the phase components of the processed SAR data and extends only the bandwidth of the magnitude, so it does not cause any phase distortion.

To apply the phase-extension inverse filtering to a real SAR image the 2-D transfer function should be shifted in the azimuth direction with Doppler centroids to divide the frequency domain more accurately, because the spectrum of the matched filtered SAR data is shifted according to Doppler centroids. And to make the signal bandwidth equal in the azimuth direction, depth of focus is carried out. Deskewing in the spatial domain is also processed. In addition, the replica pulse may be used as a range compression filter and secondary range compression may be carried out to get more accurate overall transfer function. But these additional processing is not considered in this paper. Fig. 2(a) is the 2-D overall transfer function for a point target, which is generated by simulation and is shifted by Doppler centroid value, 310Hz, in direction of azimuth frequency. And Fig. 2(b) is the spectrum of a real SAR image for test, Asanman in Korea in Fig. 3.



(a) Transfer function (b) Input Spectrum
Fig. 2. Experiment Data.



Fig. 3. Test SAR image, Asanman in Korea.

3. EXTRACTION OF IMPULSE RESPONSE AND COMPENSATION SCHEME

As an extraction method of impulse response from a real SAR image, the intensity measurement is used. For point targets two different methods, peak method and integral method, have been used to relate the scattering cross section of the point target to the received energy. In this paper we use intensity integral estimate described by

$$\tilde{\varepsilon}_i = \iint_A |v_r|^2 dA - P_{\sigma_0} A, \quad (5)$$

where v_r is signal of extracted point from a real SAR image, P_{σ_0} is space-averaged mean clutter output and A is an integral area. As the size of area is increased, the estimate is calculated. Using the convergence of the estimate according to the size of A , we verify if the extracted point from a real SAR image has the characteristics of impulse response. This intensity integral has the merits such as it does not require detailed knowledge of the system, it is insensitive to processor focus and it converges faster to the target intensity.

With the extracted impulse response we compensate the magnitudes of overall transfer function, because only the magnitudes are used in the phase-extension inverse filtering. As a simple compensation, linear interpolation is used, which is described by

$$|\hat{G}(u, v)| = (1 - \alpha) \cdot |G(u, v)| + \alpha \cdot |\tilde{G}(u, v)| \quad (6)$$

where $G(u, v)$ is the transfer function which is generated by simulation, $\tilde{G}(u, v)$ is the transfer function of the extracted point target and α is a interpolation coefficient. The value of α is determined by the convergence of the estimate in (5) and the correlation between the extracted point and the simulated impulse response.

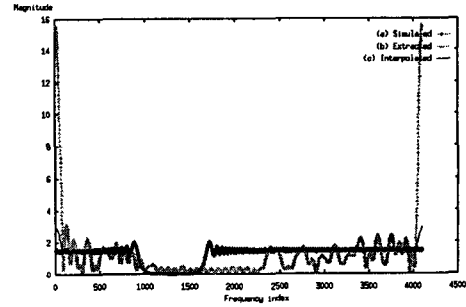


Fig. 4. Magnitudes of transfer functions.

Fig. 4 shows the magnitudes of transfer functions in direction of azimuth frequency. Line (a) is the magnitudes of simulated transfer function, (b) is the case of the extracted point and (c) is the interpolated magnitudes.

4. EXPERIMENTAL RESULT

In this section, the phase-extension inverse filtering is applied to a real SAR image. Fig. 5 shows a block diagram of reconstructing a single look complex image in a general SAR imaging system.

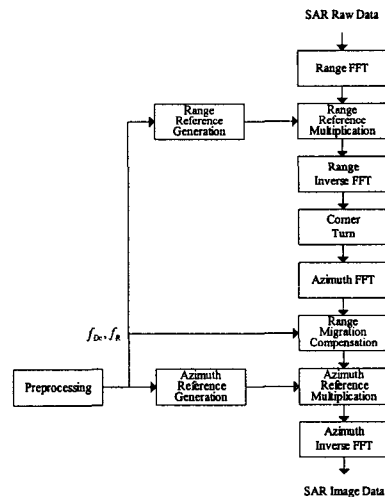


Fig. 5 Block diagram of SAR imaging algorithm.

As a test image, Fig. 3 is used. And its magnitudes of spectrum are as in Fig. 2 (a). Fig. 6 shows the result images, which are zoomed area. Fig. 6 (a) is processed with uniform weighting function, that is, no weighting. Fig. 6 (b) is the result image by phase-extension inverse filtering (PEI) with simulated transfer function and Fig 6 (c) is the case of interpolated function. And Fig. 6 (d), (e) are the result images when SVA algorithm [4] is applied to Fig. 6 (a), (c) as a post processing.

As a performance measure in real SAR processing, "image contrast" is used to examine the efficacy of the methods. Because there are clutters and the exact values

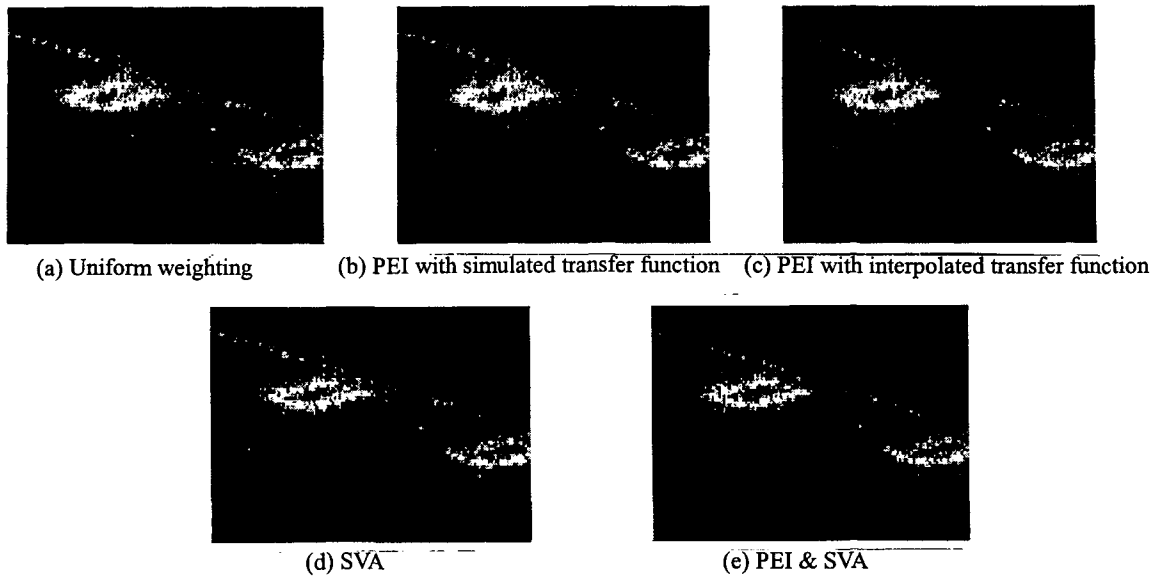


Fig. 6 Result images

of targets aren't known, image contrast is very efficient to verify the performance. The image contrast value is calculated by following equation:

$$C_s = \frac{\sqrt{\langle I^2 \rangle - \langle I \rangle^2}}{\langle I \rangle}, \quad (7)$$

where $\langle \cdot \rangle$ means the average. As image contrast value is increased, we consider that the target detectability is more improved. Table 1 shows the image contrast value of each image in Fig. 6.

Image	Image contrast
(a)	2.55
(b)	2.56
(c)	2.65
(d)	3.16
(e)	3.29

Table 1. Image contrast values

As indicated in Table I, image contrast value is increased when the phase-extension inverse filtering is applied with interpolated magnitudes of transfer function.

5. SUMMARY AND CONCLUSIONS

In this paper we examine the implementation of the phase-extension inverse filtering on a real SAR image, ERS-1 SAR image. To implement the phase-extension inverse filtering in a real environment, we consider the practical problems such as Doppler parameters. And we introduce a compensation scheme to improve the performance when the phase-extension inverse filtering is applied to a real SAR image. The result provides that

image contrast is improved. Note that the performance will be improved if the accurate transfer function can be obtained using a known reflector such as corner tone. And to get more improvement, we need to consider a complex SAR imaging environment, such as phase distortion and antenna patterns. This work will be a subject of future works.

6. ACKNOWLEDGEMENTS

The authors wish to acknowledge that this work has been partially supported by Ministry of National Defense through the Agency for Defense Development, and the author partially supported by BK21 program from Ministry of Education, Republic of Korea.

REFERENCES

- [1] J. C. Curlander and R. N. Mcdonough, *Synthetic Aperture Radar : System & Signal Processing*, John-Wiley & Sons, Inc., 1991.
- [2] D. C. Munson, JR and R. L. Visentin: "A signal processing view of strip-mapping synthetic aperture radar," *IEEE Trans. on Acoust., Speech, Signal Processing*, vol. 37, pp. 2131-2147, Dec. 1989.
- [3] S. R. DeGraaf: "SAR imaging via modern 2-D spectral estimation methods," *IEEE Trans. on Image Processing*, vol. 7, pp. 729-761, May. 1998.
- [4] H. C. Stankwitz, R. J. Dallaire, and J. R. Fienup: "Nonlinear apodization sidelobe control in SAR imagery," *IEEE Trans. on Aerosp., Electronic Systems*, vol. 31, pp. 267-279, Feb. 1982.
- [5] Dae-Won Do, Woo-Jin Song, "SAR image enhancement based on the phase extension inverse filtering", *Proceedings of ISPACS 00*, vol. 2, pp.861-864, November 2000.